Article

Stark Broadening of Al IV Spectral Lines

Milan S. Dimitrijević [1,2,*] and **Magdalena D. Christova [3]**

1   Astronomical Observatory, Volgina 7, 11060 Belgrade, Serbia
2   LERMA, Observatoire de Paris, Université PSL, CNRS, Sorbonne Université, F-92190 Meudon, France
3   Department of Applied Physics, Technical University of Sofia, 1000 Sofia, Bulgaria
*   Correspondence: mdimitrijevic@aob.rs

Abstract: Stark widths for 23 transitions in Al IV have been calculated by employing the modified semiempirical method. The results are obtained for an electron density of 10^{17} cm^{-3} and temperatures from 10,000 K to 160,000 K. The results obtained in this investigation are used for the examination of the influence of Stark broadening in Al IV stellar spectra, as well as to check the Stark width regular behavior and similarites within the Al IV spectrum.

Keywords: Stark broadening; Al IV; line profiles; atomic data; atomic processes; line formation; stellar atmospheres

1. Introduction

Data on spectral line profiles, broadened by interactions with surrounding charged particles (Stark broadening) are of interest in many research fields, such as astrophysics (e.g., [1]), laboratory plasma [2–5], inertial fusion experiments (Refs. [6,7], laser design and development [8]), laser produced plasma research [9–11] and plasmas in technology [12,13]. Particular interest for such data exists in astrophysics, where they are needed, e.g., for stellar abundance investigations, stellar atmospheres modeling, spectral lines analysis and synthesis, radiative transfer, etc.

The most interesting celestial objects for Stark brodening data applications are white dwarfs, where this is the principal pressure broadening mechanism. The importance of Stark broadening has been investigated recently in DO, DB (see e.g., [14]), DA dwarfs (see, e.g., [15]), B subdwarfs (see, e.g., [16]) and A and late B-type stars (see, e.g., [15]).

The astrophysical significance of aluminum is due to its high cosmic abundance since it is the twelfth most common element in the Universe, and its spectral lines are commonly present in stellar spectra. For example, Smiljanic et al. [17] investigated aluminum abundances in giants and dwarfs and their implications on stellar and galactic chemical evolution using two samples: (i) more than 600 dwarfs of the solar neighborhood and open clusters and (ii) low- and intermediate-mass clump giants in six open clusters. Carretta et al. [18] determined aluminum abundances for 90 red giant branch (RGB) stars in NGC 2808, and Smith [19] derrived atmospheric abundance of aluminum for a sample of forty normal, superficially normal and HgMn-type main-sequence late-B stars.

Recently, Elabidi [20] used quantum mechanical theory [21,22] to calculate 20 Al IV lines belonging to 2p^6–3s, 3s–3p and 3p–3d transitions. All of these lines are in UV, but in astronomy, they are particularly convenient spectral lines in the visible. In the case of Al IV, such lines are from 4s–4p and 4p–4d transitions, which are in Jℓ coupling. Here, using the modified semiempirical method [23], we calculated Stark widths for 23 lines and multiplets, which are all in the visible part of the spectrum, and is very convenient for astronomical observations and plasma diagnostics. The obtained results enable us to examine the influence of Stark broadening on Al IV spectral lines in DB and DO white dwarfs and A-type stars. Moreover, the similarities of Stark widths within multiplets and supermultiplets may be checked for the cas of Jℓ coupling.

2. Theory

The modified semiempirical method (MSE) has been developed for the theoretical determination of line widths and shifts of isolated spectral lines, which are emitted or absorbed by non-hydrogenic ions perturbed by their interaction with surrounding electrons. It may be particularly useful if we do not have enough atomic energy levels for the adequate application of more precise theoretical methods since for the adequate application of MSE, we need less data than for more sophysticated methods. In this formalism, the full width at half intensity maximum (FHWM) is given as [23]:

$$W_{MSE} = N \frac{8\pi}{3} \frac{\hbar^2}{m^2} \left(\frac{2m}{\pi kT}\right)^{1/2} \frac{\pi}{\sqrt{3}} \frac{\lambda^2}{2\pi c} \times$$

$$\times \Big\{ \sum_{\ell_i \pm 1} \sum_{L_{i'} J_{i'}} \vec{R}^2 [n_i \ell_i L_i J_i, n_i (\ell_i \pm 1) L_{i'} J_{i'}] \widetilde{g}(x_{\ell_i, \ell_i \pm 1}) +$$

$$+ \sum_{\ell_f \pm 1} \sum_{L_{f'} J_{f'}} \vec{R}^2 [n_f \ell_f L_f J_f, n_f (\ell_f \pm 1) L_{f'} J_{f'}] \widetilde{g}(x_{\ell_f, \ell_f \pm 1}) +$$

$$+ \Big(\sum_{i'} \vec{R}_{ii'}^2\Big)_{\Delta n \neq 0} g(x_{n_i, n_i + 1}) + \Big(\sum_{f'} \vec{R}_{ff'}^2\Big)_{\Delta n \neq 0} g(x_{n_f, n_f + 1}) \Big\}. \tag{1}$$

where the index i is the initial, and index f is the final atomic energy level. The square of the matrix element $\{\vec{R}^2[n_k \ell_k L_k J_k, (\ell_k \pm 1) L_{k'} J_{k'}], \quad k = i, f\}$ may be expressed in the following maner:

$$\vec{R}^2 [n_k \ell_k L_k J_k, n_k (\ell_k \pm 1) L_k' J_k'] =$$

$$\frac{\ell_>}{2J_k + 1} Q[\ell_k L_k, (\ell_k \pm 1) L_k'] Q(J_k, J_k') [R_{n_k^* \ell_k}^{n_k^* (\ell_k \pm 1)}]^2. \tag{2}$$

where $\ell_> = \max(\ell_k, \ell_k \pm 1)$ and

$$\Big(\sum_{k'} \vec{R}_{kk'}^2\Big)_{\Delta n \neq 0} = \Big(\frac{3n_k^*}{2Z}\Big)^2 \frac{1}{9} (n_k^{*2} + 3\ell_k^2 + 3\ell_k + 11). \tag{3}$$

In Equation (1),

$$x_{\ell_k, \ell_{k'}} = \frac{E}{\Delta E_{\ell_k, \ell_{k'}}}, \quad k = i, f$$

$E = \frac{3}{2}kT$ is the electron kinetic energy and $\Delta E_{\ell_k, \ell_{k'}} = |E_{\ell_k} - E_{\ell_{k'}}|$ is the energy difference between levels ℓ_k and $\ell_k \pm 1$ ($k = i, f$),

$$x_{n_k, n_k + 1} \approx \frac{E}{\Delta E_{n_k, n_k + 1}},$$

where $\Delta n \neq 0$, the energy difference between energy levels with n_k and $n_k + 1$, $\Delta E_{n_k, n_k + 1}$ is represented by the following equation:

$$\Delta E_{n_k, n_k + 1} = 2Z^2 E_H / n_k^{*3}, \tag{4}$$

where $n_k^* = [E_H Z^2 / (E_{ion} - E_k)]^{1/2}$ is the effective principal quantum number, N is the electron density, T is the temperature, Z the residual ionic charge (e.g., $Z = 4$ for Al IV), E_{ion} the appropriate spectral series limit, $Q(\ell L, \ell' L')$, multiplet factor and $Q(J, J')$ line factor [24]. Gaunt factors needed for calculation are denoted as $g(x)$ [25,26] and $\widetilde{g}(x)$ [23]. Radial integrals $[R_{n_k^* \ell_k}^{n_k^* \ell_k \pm 1}]$ are calculated by using the Coulomb approximation [27] with the help of tables in [28].

In some cases, these tables are not applicable, because the values are out of them, in particular, for higher principal quantum numbers, in such a case, one can use the procedure described in Ref. [29], where the case of high principal quantum numbers is elaborated.

3. Results

We calculated Stark full widths at the half intensity maximum (FWHM), by employing the modified semiempirical method [23]. The set of atomic energy levels, which need to be included as input data have been taken from [30,31]. Table 1 gives the obtained results for the electron-impact (Stark) FWHM for 23 Al IV transitions, calculated for an electron density of 10^{17} cm^{-3} and electron temperatures of 10,000, 20,000, 40,000, 80,000 and 160,000 K. Theoretical errors of our calculations are within the limit of 40 percent. Concerning the dependence of results on electron density, it is linear if the influence of Debye screening is negligible. This influence should be checked only for high densities. We draw attention to the wavelengths given in Table 1, which are not observed but calculated using atomic energy levels, so that they are not identical to the observed ones. In Table 1, is also provided the value of $3kT/2\Delta E$. This is the ratio of the mean energy of free electrons and the energy difference between the closest perturbing level and the closest of the initial and final levels (ΔE), and it emphasizes which type of collisions contribute to the line width. For values lower than one, dominate the elastic collisions. Namely, in such a case, the energy of colliding electrons is below the threshold for excitation of atomic energy levels. When it increases above this value, the contribution of inelastic collisions increases.

From the first work in 1980 [23], MSE has been applied and checked many times (see, e.g., [32], and references therein). In order to test this method, selected experimental data for 36 multiplets (seven different ion species) of triply charged ions were compared [23] with theoretical linewidths. The averaged values of the ratios of measured to calculated widths for doubly charged ions were 1.06 ± 0.32 and for triply charged ions 0.91 ± 0.42. Since for complex spectra, the agreement may be worse, we assumed that the average accuracy is within the limits of about $\pm 50\%$, but it has been shown [33,34] that the MSE approach, even in the case of emitters with complex spectra (e.g., Xe II and Kr II), gives very good agreement with experimental measurements (in the interval $\pm 30\%$). For example, for the 6s–6p transitions of Xe II, the averaged ratio between the experimental and theoretical widths of the lines is 1.15 ± 0.5 [33]. Consequently, we assume that the average accuracy of the results obtained here for Al IV is not worse than 40%.

There is no experimental or other theoretical data for Stark broadening of Al IV transitions investigated here.

The results presented here for Al IV Stark widths are from six multiplets, three belonging to the spectral series with parent term $^2P^o_{1/2}$: 4s $^2[1/2]^o$–4p $^2[1/2]$, 4s $^2[1/2]^o$–4p $^2[3/2]$ and 4p $^2[1/2]$–4d $^2[3/2]^o$, and three belonging to the spectral series with parent term $^2P^o_{3/2}$: 4s $^2[3/2]^o$–4p $^2[1/2]$, 4p $^2[1/2]$–4d $^2[1/2]^o$, and 4p $^2[1/2]$–4d $^2[3/2]^o$. We have also four supermultiplets: 4s $^2[K]^o$–4p $^2[K']$ and 4p $^2[K]$–4d $^2[K']^o$, in spectral series with parent terms $^2P^o_{1/2}$ and $^2P^o_{3/2}$. This gives us an opportunity to check similarities of Stark widths within the present Al IV multiplets and supermultiplets. Namely, when such similarities are present, this may be used, for example, to check whether the existing experimental or theoretical values are consistent, and also to use existing data to estimate needed line widths, which are unknown.

Table 1. FWHM (full widths at half intensity maximum) (W) for Al IV spectral lines broadened by impacts with surrounding electrons, for an electron density of 10^{17} cm^{-3} and temperatures from 10,000 K to 160,000 K.

Transition	T (K)	W (Å)	3kT/2ΔE
Al IV $2s^22p^5(^2P^o_{1/2})4s\ ^2[1/2]^o$–$2s^22p^5(^2P^o_{1/2})4p\ ^2[1/2]_1$	10,000	1.07	0.471
	20,000	0.754	0.942
$\lambda = 4515.6$ Å	40,000	0.533	1.88
	80,000	0.410	3.77
	160,000	0.352	7.53
Al IV $2s^22p^5(^2P^o_{1/2})4s\ ^2[1/2]^o$–$2s^22p^5(^2P^o_{1/2})4p\ ^2[1/2]_0$	10,000	0.643	0.471
	20,000	0.455	0.942
$\lambda = 3261.3$ Å	40,000	0.322	1.88
	80,000	0.250	3.77
	160,000	0.215	7.53
Al IV $2s^22p^5(^2P^o_{1/2})4s\ ^2[1/2]^o$–$2s^22p^5(^2P^o_{1/2})4p\ ^2[3/2]$	10,000	2.00	0.471
	20,000	1.42	0.943
$\lambda = 4520.2$ Å	40,000	1.00	1.89
	80,000	0.776	3.77
	160,000	0.671	7.54
Al IV $2s^22p^5(^2P^o_{1/2})4p\ ^2[1/2]_1$–$2s^22p^5(^2P^o_{1/2})4d\ ^2[3/2]^o_2$	10,000	0.747	2.36
	20,000	0.554	4.73
$\lambda = 3485.1$ Å	40,000	0.429	9.45
	80,000	0.345	18.9
	160,000	0.296	37.8
Al IV $2s^22p^5(^2P^o_{1/2})4p\ ^2[1/2]_1$–$2s^22p^5(^2P^o_{1/2})4d\ ^2[3/2]^o_1$	10,000	0.710	3.99
	20,000	0.543	7.98
$\lambda = 3279.5$ Å	40,000	0.422	16.0
	80,000	0.340	31.9
	160,000	0.294	63.8
Al IV $2s^22p^5(^2P^o_{1/2})4p\ ^2[1/2]_0$–$2s^22p^5(^2P^o_{1/2})4d\ ^2[3/2]^o_1$	10,000	1.38	3.99
	20,000	1.05	7.98
$\lambda = 4550.5$ Å	40,000	0.817	16.0
	80,000	0.659	31.9
	160,000	0.571	63.8
Al IV $2s^22p^5(^2P^o_{1/2})4p\ ^2[3/2]$–$2s^22p^5(^2P^o_{1/2})4d\ ^2[5/2]^o$	10,000	0.506	2.32
	20,000	0.381	4.64
$\lambda = 3492.1$ Å	40,000	0.303	9.28
	80,000	0.248	18.6
	160,000	0.213	37.1
Al IV $2s^22p^5(^2P^o_{1/2})4p\ ^2[3/2]_1$–$2s^22p^5(^2P^o_{1/2})4d\ ^2[3/2]^o_2$	10,000	0.780	2.36
	20,000	0.578	4.73
$\lambda = 3482.3$ Å	40,000	0.446	9.45
	80,000	0.358	18.9
	160,000	0.307	37.8
Al IV $2s^22p^5(^2P^o_{1/2})4p\ ^2[3/2]_1$–$2s^22p^5(^2P^o_{1/2})4d\ ^2[3/2]^o_1$	10,000	0.741	3.99
	20,000	0.565	7.98
$\lambda = 3277.0$ Å	40,000	0.437	16.0
	80,000	0.352	31.9
	160,000	0.305	63.8

Table 1. *Cont.*

Transition	T (K)	W (Å)	3kT/2ΔE
Al IV $2s^22p^5(^2P^o_{3/2})4s$ $^2[3/2]^o$–$2s^22p^5(^2P^o_{3/2})4p$ $^2[1/2]_1$	10,000	1.33	0.545
	20,000	0.940	1.09
$\lambda = 5224.1$ Å	40,000	0.668	2.18
	80,000	0.520	4.36
	160,000	0.448	8.72
Al IV $2s^22p^5(^2P^o_{3/2})4s$ $^2[3/2]^o$–$2s^22p^5(^2P^o_{3/2})4p$ $^2[1/2]_0$	10,000	0.830	0.545
	20,000	0.587	1.09
$\lambda = 3916.5$ Å	40,000	0.415	2.18
	80,000	0.320	4.36
	160,000	0.276	8.72
Al IV $2s^22p^5(^2P^o_{3/2})4s$ $^2[3/2]^o$–$2s^22p^5(^2P^o_{3/2})4p$ $^2[3/2]$	10,000	0.684	0.545
	20,000	0.484	1.09
$\lambda = 4291.9$ Å	40,000	0.342	2.18
	80,000	0.263	4.36
	160,000	0.225	8.72
Al IV $2s^22p^5(^2P^o_{3/2})4s$ $^2[3/2]^o$–$2s^22p^5(^2P^o_{3/2})4p$ $^2[5/2]$	10,000	0.606	0.545
	20,000	0.429	1.09
$\lambda = 4544.1$ Å	40,000	0.303	2.18
	80,000	0.232	4.36
	160,000	0.198	8.72
Al IV $2s^22p^5(^2P^o_{3/2})4p$ $^2[1/2]_1$–$2s^22p^5(^2P^o_{3/2})4d$ $^2[1/2]^o$	10,000	0.589	1.89
	20,000	0.441	3.77
$\lambda = 3279.6$ Å	40,000	0.348	7.55
	80,000	0.287	15.1
	160,000	0.249	30.2
Al IV $2s^22p^5(^2P^o_{3/2})4p$ $^2[1/2]_1$–$2s^22p^5(^2P^o_{3/2})4d$ $^2[3/2]^o$	10,000	0.387	2.71
	20,000	0.294	5.43
$\lambda = 3108.0$ Å	40,000	0.236	10.9
	80,000	0.195	21.7
	160,000	0.166	43.4
Al IV $2s^22p^5(^2P^o_{3/2})4p$ $^2[1/2]_0$–$2s^22p^5(^2P^o_{3/2})4d$ $^2[1/2]^o$	10,000	0.977	1.89
	20,000	0.731	3.77
$\lambda = 4210.3$ Å	40,000	0.575	7.55
	80,000	0.474	15.1
	160,000	0.412	30.2
Al IV $2s^22p^5(^2P^o_{3/2})4p$ $^2[1/2]_0$–$2s^22p^5(^2P^o_{3/2})4d$ $^2[3/2]^o$	10,000	0.624	2.71
	20,000	0.473	5.43
$\lambda = 3931.7$ Å	40,000	0.381	10.9
	80,000	0.313	21.7
	160,000	0.267	43.4
Al IV $2s^22p^5(^2P^o_{3/2})4p$ $^2[3/2]$–$2s^22p^5(^2P^o_{3/2})4d$ $^2[1/2]^o$	10,000	0.829	1.89
	20,000	0.619	3.77
$\lambda = 3797.4$ Å	40,000	0.485	7.55
	80,000	0.399	15.1
	160,000	0.347	30.2
Al IV $2s^22p^5(^2P^o_{3/2})4p$ $^2[3/2]$–$2s^22p^5(^2P^o_{3/2})4d$ $^2[3/2]^o$	10,000	0.546	2.71
	20,000	0.412	5.43
$\lambda = 3569.2$ Å	40,000	0.329	10.9
	80,000	0.270	21.7
	160,000	0.231	43.4

Table 1. *Cont.*

Transition	T (K)	W (Å)	3kT/2ΔE
Al IV $2s^2 2p^5(^2P^o_{3/2})4p\ ^2[3/2]$–$2s^2 2p^5(^2P^o_{3/2})4d\ ^2[5/2]^o$	10,000	0.704	2.94
	20,000	0.540	5.88
$\lambda = 3532.0$ Å	40,000	0.437	11.8
	80,000	0.363	23.5
	160,000	0.310	47.0
Al IV $2s^2 2p^5(^2P^o_{3/2})4p\ ^2[5/2]$–$2s^2 2p^5(^2P^o_{3/2})4d\ ^2[3/2]^o$	10,000	0.372	2.71
	20,000	0.278	5.43
$\lambda = 3411.8$ Å	40,000	0.217	10.9
	80,000	0.176	21.7
	160,000	0.149	43.4
Al IV $2s^2 2p^5(^2P^o_{3/2})4p\ ^2[5/2]$–$2s^2 2p^5(^2P^o_{3/2})4d\ ^2[5/2]^o$	10,000	0.458	2.94
	20,000	0.347	5.88
$\lambda = 3377.7$ Å	40,000	0.276	11.8
	80,000	0.226	23.5
	160,000	0.192	47.0
Al IV $2s^2 2p^5(^2P^o_{3/2})4p\ ^2[5/2]$–$2s^2 2p^5(^2P^o_{3/2})4d\ ^2[7/2]^o$	10,000	0.511	2.10
	20,000	0.381	4.20
$\lambda = 3499.1$ Å	40,000	0.295	8.39
	80,000	0.238	16.8
	160,000	0.204	33.6

Wiese and Konjević [35] found, by analyzing experimental data from the literature, that if we express Stark widths in angular frequency units, differences within the same multiplet should usually not exceed several percent, and about 30 percent in the case of a supermultiplet. It is interesting to check this for the Al IV transitions presented here, which are in the Jℓ coupling scheme. In oder to do this, we present in Table 2 Stark widths expressed in Ångströms and angular frequency units for T = 80,000 K since this temperature is closest to the middle of the investigated interval of temperatures.

For the transformation of Stark widths between Å and angular frequency units, one can use the following relation:

$$W(\mathring{A}) = \frac{\lambda^2}{2\pi c} W(s^{-1}), \tag{5}$$

where c is the speed of light.

If we analyze the data in Table 2, we can see that in the spectral series with parent term $^2P^o_{1/2}$, in the case of multiplet $4s\ ^2[1/2]^o$–$4p\ ^2[1/2]$, the greatest width is 64% larger than the smallest one if expressed in Ångströms and 17% if the widths are in angular frequency units. For the $4p\ ^2[1/2]$–$4d\ ^2[3/2]^o$ multiplet, these values are 94% and 12%, and for $4p\ ^2[3/2]$–$4d\ ^2[3/2]^o$ 1.7% and 11%, respectively. For the spectral series with parent term $^2P^o_{3/2}$, these values are 62.5% and 9.5% in the case of the $4s\ ^2[3/2]^o$–$4p\ ^2[1/2]$ multiplet, 65% and 0.4% for the $4p\ ^2[1/2]$–$4d\ ^2[1/2]^o$ multiplet, and 60.5% and 0.5% for the $4p\ ^2[1/2]$–$4d\ ^2[3/2]^o$ multiplet.

We can see that for the considered Al IV transition in the Jℓ coupling, these differences may be of the order of 10–20 percent if expressed in angular frequency units, which enables a rough check of consistency of existing experimental and theoretical data or an approximate check during experiment or calculation.

In the case of supermultiplet $4s\ ^2[K]^o$–$4p\ ^2[K']$, belonging to the spectral series with parent term $^2P^o_{1/2}$, the maximal difference when the line width is expressed in Ångströms, is 210% and 89% if the widths are in angular frequency units. For the $4p\ ^2[K]$–$4d\ ^2[K']^o$ supermultiplet, which belongs to the same spectral series, these values are 166% and 61%. The similar situation is for supermultiplets in spectral series with the parent term $^2P^o_{3/2}$.

For supermultiplet 4s ^{2}[K]^o–4p ^{2}[K'], these values are 124% and 85%, respectively, while for 4p ^{2}[K]–4d ^{2}[K']^o, they are 169% and 93%. We can see that the prediction [35] that the differences of Stark widths in angular frequency units, within the same supermultiplet usually does not exceed about 30 percent, in the case of Al IV transition in Jℓ coupling, considered here, is not satisfied.

Table 2. Electron-impact broadening (Stark broadening), full widths at half intensity maximum (W) in (Å) and (10^{12} s^{-1}) for Al IV spectral lines, for an electron density of 10^{17} cm^{-3} and T = 80,000 K.

Transition	λ (Å)	W (Å)	W (10^{12} s^{-1})
Al IV 2s^{2}2p^5(^{2}P$^o_{1/2}$)4s ^{2}[1/2]^o–2s^{2}2p^5(^{2}P$^o_{1/2}$)4p ^{2}[1/2]$_1$	4516	0.410	0.379
Al IV 2s^{2}2p^5(^{2}P$^o_{1/2}$)4s ^{2}[1/2]^o–2s^{2}2p^5(^{2}P$^o_{1/2}$)4p ^{2}[1/2]$_0$	3261	0.250	0.442
Al IV 2s^{2}2p^5(^{2}P$^o_{1/2}$)4s ^{2}[1/2]^o–2s^{2}2p^5(^{2}P$^o_{1/2}$)4p ^{2}[3/2]	4520	0.776	0.715
Al IV 2s^{2}2p^5(^{2}P$^o_{1/2}$)4p ^{2}[1/2]$_1$–2s^{2}2p^5(^{2}P$^o_{1/2}$)4d ^{2}[3/2]$^o_2$	3485	0.345	0.535
Al IV 2s^{2}2p^5(^{2}P$^o_{1/2}$)4p ^{2}[1/2]$_1$–2s^{2}2p^5(^{2}P$^o_{1/2}$)4d ^{2}[3/2]$^o_1$	3279	0.340	0.596
Al IV 2s^{2}2p^5(^{2}P$^o_{1/2}$)4p ^{2}[1/2]$_0$–2s^{2}2p^5(^{2}P$^o_{1/2}$)4d ^{2}[3/2]$^o_1$	4551	0.659	0.599
Al IV 2s^{2}2p^5(^{2}P$^o_{1/2}$)4p ^{2}[3/2]–2s^{2}2p^5(^{2}P$^o_{1/2}$)4d ^{2}[5/2]^o	3492	0.248	0.383
Al IV 2s^{2}2p^5(^{2}P$^o_{1/2}$)4p ^{2}[3/2]$_1$–2s^{2}2p^5(^{2}P$^o_{1/2}$)4d ^{2}[3/2]$^o_2$	3482	0.358	0.556
Al IV 2s^{2}2p^5(^{2}P$^o_{1/2}$)4p ^{2}[3/2]$_1$–2s^{2}2p^5(^{2}P$^o_{1/2}$)4d ^{2}[3/2]$^o_1$	3277	0.352	0.618
Al IV 2s^{2}2p^5(^{2}P$^o_{3/2}$)4s ^{2}[3/2]^o–2s^{2}2p^5(^{2}P$^o_{3/2}$)4p ^{2}[1/2]$_1$	5224	0.520	0.359
Al IV 2s^{2}2p^5(^{2}P$^o_{3/2}$)4s ^{2}[3/2]^o–2s^{2}2p^5(^{2}P$^o_{3/2}$)4p ^{2}[1/2]$_0$	3917	0.320	0.393
Al IV 2s^{2}2p^5(^{2}P$^o_{3/2}$)4s ^{2}[3/2]^o–2s^{2}2p^5(^{2}P$^o_{3/2}$)4p ^{2}[3/2]	4292	0.263	0.269
Al IV 2s^{2}2p^5(^{2}P$^o_{3/2}$)4s ^{2}[3/2]^o–2s^{2}2p^5(^{2}P$^o_{3/2}$)4p ^{2}[5/2]	4544	0.232	0.212
Al IV 2s^{2}2p^5(^{2}P$^o_{3/2}$)4p ^{2}[1/2]$_1$–2s^{2}2p^5(^{2}P$^o_{3/2}$)4d ^{2}[1/2]^o	3280	0.287	0.502
Al IV 2s^{2}2p^5(^{2}P$^o_{3/2}$)4p ^{2}[1/2]$_1$–2s^{2}2p^5(^{2}P$^o_{3/2}$)4d ^{2}[3/2]^o	3108	0.195	0.380
Al IV 2s^{2}2p^5(^{2}P$^o_{3/2}$)4p ^{2}[1/2]$_0$–2s^{2}2p^5(^{2}P$^o_{3/2}$)4d ^{2}[1/2]^o	4210	0.474	0.504
Al IV 2s^{2}2p^5(^{2}P$^o_{3/2}$)4p ^{2}[1/2]$_0$–2s^{2}2p^5(^{2}P$^o_{3/2}$)4d ^{2}[3/2]^o	3932	0.313	0.382
Al IV 2s^{2}2p^5(^{2}P$^o_{3/2}$)4p ^{2}[3/2]–2s^{2}2p^5(^{2}P$^o_{3/2}$)4d ^{2}[1/2]^o	3797	0.399	0.521
Al IV 2s^{2}2p^5(^{2}P$^o_{3/2}$)4p ^{2}[3/2]–2s^{2}2p^5(^{2}P$^o_{3/2}$)4d ^{2}[3/2]^o	3569	0.270	0.400
Al IV 2s^{2}2p^5(^{2}P$^o_{3/2}$)4p ^{2}[3/2]–2s^{2}2p^5(^{2}P$^o_{3/2}$)4d ^{2}[5/2]^o	3532	0.363	0.548
Al IV 2s^{2}2p^5(^{2}P$^o_{3/2}$)4p ^{2}[5/2]–2s^{2}2p^5(^{2}P$^o_{3/2}$)4d ^{2}[3/2]^o	3412	0.176	0.284
Al IV 2s^{2}2p^5(^{2}P$^o_{3/2}$)4p ^{2}[5/2]–2s^{2}2p^5(^{2}P$^o_{3/2}$)4d ^{2}[5/2]^o	3378	0.226	0.373
Al IV 2s^{2}2p^5(^{2}P$^o_{3/2}$)4p ^{2}[5/2]–2s^{2}2p^5(^{2}P$^o_{3/2}$)4d ^{2}[7/2]^o	3499	0.238	0.366

4. On the Stark Broadening in Stellar Atmospheres

The obtained results are used here to show the influence of electron impacts on Al IV lines (Stark broadening) in stellar spectra. Recently, we performed a similar investigation for Zn III spectral lines in the UV part of the spectrum [36]. For the A-type stellar atmosphere, we found that Doppler width was dominant for all considered Rosseland optical depths and that the Stark broadening could be neglected. For the DB white dwarf atmosphere, Stark width was dominant for all investigated Rosseland optical depths, while for the DO white dwarf case, Stark broadening was dominant for higher values of Rosseland optical depth, while for lower ones, Doppler broadening was higher, but in most cases, comparable to the Stark broadening.

In order to demonstrate the influence of Stark broadening on the Al IV spectral lines considered here, which are all in the visible part of the spectrum, as a difference from Zn III UV lines, we compared Stark and Doppler widths for different Rosseland optical depths, taking into account the transition with the largest (2s^{2}2p^5(^{2}P$^o_{1/2}$)4s ^{2}[1/2]^o–2s^{2}2p^5(^{2}P$^o_{1/2}$)4p ^{2}[3/2], λ = 4250.2 Å) and the smallest (2s^{2}2p^5(^{2}P$^o_{3/2}$)4p ^{2}[5/2]–2s^{2}2p^5(^{2}P$^o_{3/2}$)4d ^{2}[3/2]^o, λ = 3411.8 Å) Stark width values from Table 1.

Figure 1 presents ratios of Stark and Doppler widths for an A-type star atmospheric model with effective temperature T$_{eff}$ = 8500 K and logarithm of surface gravity log g = 4.5 [37]. As a difference from UV Zn III lines, in the case of Al IV lines in the visible, for higher values of Rosseland opacity or deeper atmospheric layers, Stark broadening may be a correction that increases the accuracy. In Figure 2, such an analysis is performed for a

model of the DB white dwarf atmosphere with T_{eff} = 25,000 K and log g = 8.0 [38]. One can see that for such an atmospheric model, Stark width is dominant for both transitions and for all investigated Rosseland optical depths, even more than in the case of the previously investigated Zn III UV multiplets. For the DO white dwarf atmosphere model with T_{eff} = 60,000 K and log g = 8.0 [38] (see Figure 3), we can see the difference in the influence of Stark broadening on UV and optical spectral lines. Namely, differently from UV Zn III lines, in the case of Al IV, Stark broadening dominates for both transitions and for all Rosseland optical depths of interest.

    This illustrates the influence of wavelength values. Namely, in Stark broadening theories, the wavelength enters as a square and the expression for Doppler width is linear with wavelength. Therefore, with the increase of wavelength, Stark widths increase faster than Doppler ones. Thus, in the visible part of the spectrum, the influence of Stark broadening will be higher in comparison with Doppler broadening, than in the UV part.
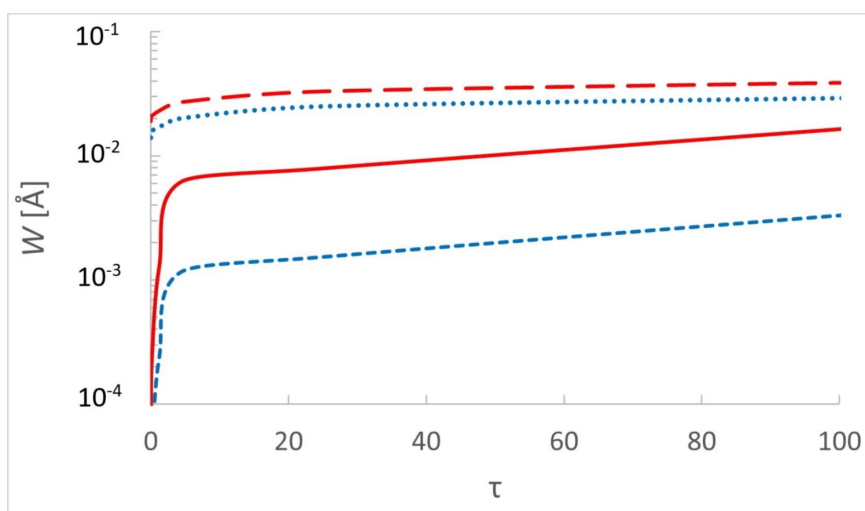
Figure 1. Dependence of Stark and Doppler full widths at half intensity maximum of Al IV $2s^22p^5(^2P^o_{1/2})4s\ ^2[1/2]^o - 2s^22p^5(^2P^o_{1/2})4p\ ^2[3/2]0$, λ = 4520.2 Å (red, Stark$-$solid line, Doppler$-$long dashes) and $2s^22p^5(^2P^o_{3/2})4p\ ^2[5/2] - 2s^22p^5(^2P^o_{3/2})4d\ ^2[3/2]^o$, λ = 3411.8 Å (blue, Stark$-$dashes, Doppler$-$dots) spectral lines, on the Rosseland optical depth in the atmosphere of an A$-$type star. Model of stellar atmosphere [37] with parameters T_{eff} = 8500 K and log g = 4.5.
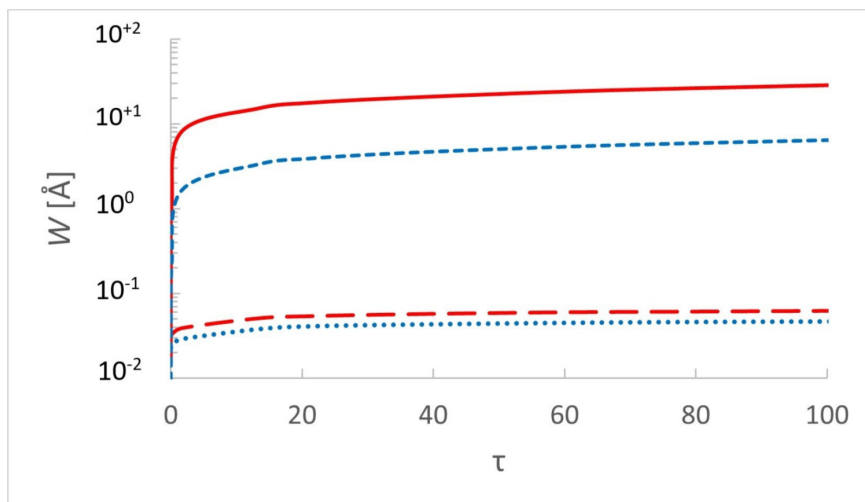
Figure 2. Same as in Figure 1 but for the atmosphere of a DB white dwarf. The atmosphere model from [38] with parameters T_{eff} = 25,000 K and log g = 8.
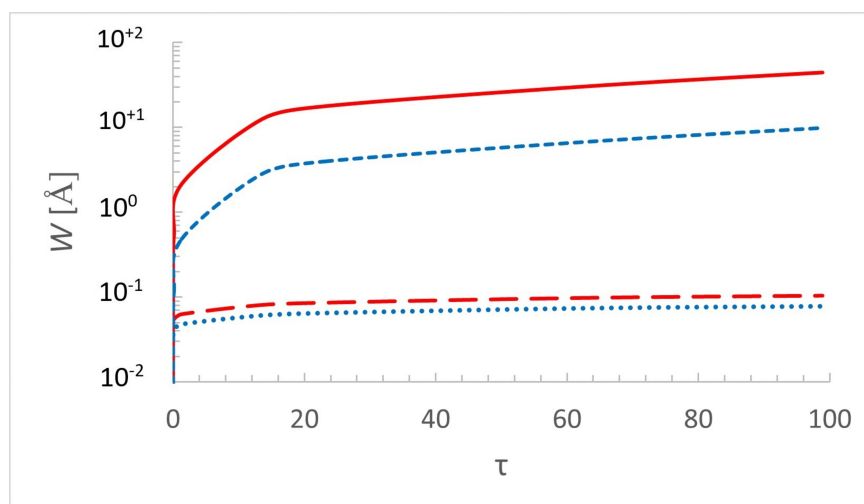
Figure 3. Same as in Figure 1 but for the atmosphere of a DO white dwarf. The atmosphere model from [38] with parameters T_{eff} = 60,000 K and log g = 8.

5. Conclusions

We calculated Stark widths for 23 Al IV transitions in Jℓ coupling, with the help of the modified semiempirical method [23]. For the considered transitions, which are all in the visible part of the spectrum, there are no other experimental or theoretical data. With the help of the obtained data, we investigated the influence of Stark broadening on Al IV spectral lines in the visible part of the spectrum, in the atmospheres of A-type stars and DB and DO white dwarfs. In comparison with lines in UV, the influence of Stark broadening in the visible part of the spectrum is higher due to the influence of higher wavelengths. We also used the obtained results to check regularities and similarities among Al IV Stark widths within multiplets and supermultiplets and found that in the case of Jℓ coupling (investigated here), differences of Stark widths within multiplets of Al IV transitions considered here are 10–20 percent, while within investigated supermultiplets, there are no similarities which would be useful for the check of consistency of experimental or theoretical results.

The Al IV Stark widths presented in this article will also be entered into the STARK-B database (http://stark-b.obspm.fr/ (accessed on 27 January 2023), Refs. [39,40], in the Virtual Atomic and Molecular Data Center VAMDC (http://www.vamdc.org/ (accessed on 27 January 2023), Refs. [41,42]).

The presented spectral line widths of Al IV, broadened by collisions with surrouning electrons (Stark broadening) may be used for many topics in astrophysics such as the modeling of stellar atmospheres, abundance determination of aluminium, analysis and synthesis of Al IV lines in stellar spectra, opacity calculations, investigation, modeling and diagnostics of laboratory plasmas as well as for various technological applications, in particular, for the optimization of cutting, welding, melting and piercing of aluminum by lasers. They also may be used for the diagnostic and modeling of an electrodynamic macro-particle accelerator arc plasma created by the evaporation of an Al-foil [43,44] and for diagnostics of plasmas generated during incipient laser ablation of aluminum in air [45].

Author Contributions: All authors were involved in the preparation of the manuscript. All authors have read and agreed to the published version of the manuscript.

Institutional Review Board Statement: Not applicable.

Informed Consent Statement: Not applicable.

Data Availability Statement: All obtained data are in the paper.

Conflicts of Interest: The authors declare no conflict of interest.

References

1. Beauchamp, A.; Wesemael, F.; Bergeron, P. Spectroscopic Studies of DB White Dwarfs: Improved Stark Profiles for Optical Transitions of Neutral Helium. *Astrophys. J. Suppl. Ser.* **1997**, *108*, 559–573. [CrossRef]
2. Konjević, N. Plasma broadening and shifting of non-hydrogenic spectral lines: Present status and applications. *Phys. Rep.* **1999**, *316*, 339–401. [CrossRef]
3. Torres, J.; van de Sande, M.J.; van der Mullen, J.J.A.M.; Gamero, A.; Sola, A. Stark broadening for simultaneous diagnostics of the electron density and temperature in atmospheric microwave discharges. *Spectrochim. Acta B* **2006**, *61*, 58–68. [CrossRef]
4. Belostotskiy, S.G.; Ouk, T.; Donnelly, V.M.; Economou, D.J.; Sadeghi, N.J. Gas temperature and electron density profiles in an argon dc microdischarge measured by optical emission spectroscopy. *Appl. Phys.* **2010**, *107*, 053305. [CrossRef]
5. Zhou, Y.; Li, H.; Jung, J.-E.J.; Ki, N.S.; Donnelly, V.M. Effects of N_2 and O_2 plasma treatments of quartz surfaces exposed to H_2 plasmas. *J. Vac. Sci. Technol. A* **2022**, *40*, 053002. [CrossRef]
6. Griem, H.R. Plasma spectroscopy in inertial confinement fusion and soft X-ray laser research. *Phys. Fluids* **1992**, *4*, 2346–2361. [CrossRef]
7. Iglesias, E.; Griem, H.R.; Welch, B.; Weaver, J. UV Line Profiles of B V from a 10-Ps KrF-Laser-Produced Plasma. *Astrophys. Space Sci.* **1997**, *256*, 327–331. [CrossRef]
8. Wang, J.S.; Griem, H.R.; Huang, Y.W.; Böttcher, F. Measurements of line broadening of B V Hα and Lδ in a laser-produced plasma. *Phys. Rev. A* **1992**, *45*, 4010–4014. [CrossRef]
9. Gornushkin, I.B.; King, L.A.; Smith, B.W.; Omenetto, N.; Winefordner, J.D. Line broadening mechanisms in the low pressure laser-induced plasma. *Spectrochim. Acta* **1999**, *54*, 1207–1217. [CrossRef]
10. Nicolosi, P.; Garifo, L.; Jannitti, E.; Malvezzi, A.M.; Tondello, G. Broadening and self-absorption of the resonance lines of H-like light ions in laser-produced plasmas. *Nuovo Cim. B* **1978**, *48*, 133–151. [CrossRef]
11. Sorge, S.; Wierling, A.; Röpke, G.; Theobald, W.; Suerbrey, R.; Wilhein, T. Diagnostics of a laser-induced dense plasma by hydrogen-like carbon spectra. *J. Phys. B* **2000**, *33*, 2983–3000. [CrossRef]
12. Yilbas, B.S.; Patel, F.; Karatas, C. Laser controlled melting of H12 hot-work tool steel with B_4C particles at the surface. *Opt. Laser Technol.* **2015**, *74*, 36–42. [CrossRef]
13. Hoffman, J.; Szymański, Z.; Azharonok, V. Laser controlled melting of H12 hot-work tool steel with B4C particles at the surface. *AIP Conf. Proc.* **2006**, *812*, 469–472.
14. Dimitrijević, M.S.; Christova, M.D. Stark widths of Lu II spectral lines. *Eur. Phys. J. D* **2021**, *75*, 172. [CrossRef]
15. Majlinger, Z.; Dimitrijević, M.S.; Srećković, V. Stark broadening of Zr IV spectral lines in the atmospheres of chemically peculiar stars. *Mon. Not. R. Astron. Soc.* **2020**, *470*, 1911–1918. [CrossRef]
16. Hamdi, R.; Ben Nessib, N.; Milovanović, N.; Popović, L.Č.; Dimitrijević, M.S.; Sahal-Bréchot, S. Stark Widths of Ar II Spectral Lines in the Atmospheres of Subdwarf B Stars. *Atoms* **2017**, *5*, 26. [CrossRef]
17. Smiljanic, R.; Romano, D.; Bragaglia, A.; Donati, P.; Magrini, L.A.U.R.A.; Friel, E.; Jacobson, H.; Randich, S.; Ventura, P.; Lind, K.; et al. The Gaia -ESO Survey: Sodium and aluminium abundances in giants and dwarfs. Implications for stellar and Galactic chemical evolution. *Astron. Astrophys.* **2016**, *589*, A115. [CrossRef]
18. Carretta, E.; Bragaglia, A.; Lucatello, S.; Gratton, R.G.; D'Orazi, V.; Sollima, A. Aluminium abundances in five discrete stellar populations of the globular cluster NGC 2808. *Astron. Astrophys.* **2018**, *615*, A17. [CrossRef]
19. Smith, K.C.; Elemental abundances in normal late-B and HgMn stars from co-added IUE spectra II. Magnesium, aluminium and silicon. *Astron. Astrophys.* **1993**, *276*, 393–408.
20. Elabidi, H. Systematic trends of Stark broadening parameters with spectroscopic charge Z within the neon isoelectronic sequence from Mg III to Br XXVI. *J. Quant. Spectrosc. Radiat. Transf.* **2021**, *259*, 107407. [CrossRef]
21. Elabidi, H.; Ben Nessib, N.; Sahal-Bréchot, S. Quantum mechanical calculations of the electron-impact broadening of spectral lines for intermediate coupling. *J. Phys. B* **2004**, *37*, 63–71. [CrossRef]
22. Elabidi, H.; Ben Nessib, N.; Cornille, M.; Dubau, J.; Sahal-Bréechot, S. Electron impact broadening of spectral lines in Be-like ions: Quantum calculations. *J. Phys. B* **2008**, *41*, 025702. [CrossRef]
23. Dimitrijević, M.S.; Konjević, N. Stark widths of doubly- and triply-ionized atom lines. *J. Quant. Spectrosc. Radiat. Transf.* **1980**, *24*, 451–459 . [CrossRef]
24. Shore, B.W.; Menzel, D. Generalized Tables for the Calculation of Dipole Transition Probabilities. *Astrophys. J. Suppl. Ser.* **1965**, *12*, 187–214. [CrossRef]
25. Griem, H.R. Semiempirical Formulas for the Electron-Impact Widths and Shifts of Isolated Ion Lines in Plasmas. *Phys. Rev.* **1968**, *165*, 258–266. [CrossRef]
26. Griem, H.R. *Spectral Line Broadening by Plasmas*; McGraw-Hill: New York, NY, USA, 1974.

27. Bates, D.R.; Damgaard, A. The Calculation of the Absolute Strengths of Spectral Lines. *Philos. Trans. R. Soc. Lond. Ser. A* **1949**, *242*, 101–122.
28. Oertel, G.K.; Shomo, L.P. Tables for the Calculation of Radial Multipole Matrix Elements by the Coulomb Approximation. *Astrophys. J. Suppl. Ser.* **1968**, *16*, 175–218. [CrossRef]
29. Van Regemorter, H.; Dy Hoang, B.; Prud'homme, M. Radial transition integrals involving low or high effective quantum numbers in the Coulomb approximation. *J. Phys. B* **1979**, *12*, 1053–1061. [CrossRef]
30. Martin, W.C.; Zalubas, R. Energy Levels of Aluminium, Al I through Al XIII. *J. Phys. Chem. Ref. Data* **1979**, *8*, 817–864. [CrossRef]
31. Kramida, A.; Ralchenko, Y.; Reader, J. NIST ASD Team. *NIST Atomic Spectra Database*, Version 5.10; National Institute of Standards and Technology: Gaithersburg, MD, USA, 2021. Available online: https://physics.nist.gov/asd (accessed on 20 January 2023).
32. Dimitrijević, M.S. Forty Years of the Applications of Stark Broadening Data Determined with the Modified Semiempirical Method. *Data* **2020**, *5*, 73. [CrossRef]
33. Popović, L.Č; Dimitrijević, M.S. Stark broadening of Xe II lines. *Astron. Astrophys. Suppl. Ser.* **1996**, *116*, 359. [CrossRef]
34. Popović, L.Č; Dimitrijević, M.S. Stark broadening parameters for Kr II lines from 5s-5p transitions. *Astron. Astrophys. Suppl. Ser.* **1998**, *127*, 295. [CrossRef]
35. Wiese, W.L.; Konjević, N. Regularities and similarities in plasma broadened spectral line widths (Stark widths). *J. Quant. Spectrosc. Radiat. Transf.* **1982**, *28*, 185–198. [CrossRef]
36. Dimitrijević, M.S.; Christova, M.D. Stark Broadening of Zn III Spectral Lines. *Universe* **2022**, *8*, 430. [CrossRef]
37. Kurucz, R.L. Model atmospheres for G, F, A, B, and O stars. *Astrophys. J. Suppl. Ser.* **1979**, *40* 1–340. [CrossRef]
38. Wesemael, F. Atmospheres for hot, high-gravity stars. II. Pure helium models. *Astrophys. J. Suppl. Ser.* **1981**, *45* 177–257. [CrossRef]
39. Sahal-Bréchot, S.; Dimitrijević, M.S.; Moreau, N.; Ben Nessib, N. The STARK-B database VAMDC node: A repository for spectral line broadening and shifts due to collisions with charged particles. *Phys. Scr.* **2015**, *90*, 054008. [CrossRef]
40. Sahal- Bréchot, S.; Dimitrijević, M.S.; Moreau, N. STARK-B Database. Available online: http://stark-B.obspm.fr (accessed on 27 January 2023).
41. Dubernet, M.L.; Antony, B.K.; Ba, Y.A.; Babikov, Y.L.; Bartschat, K.; Boudon, V.; Braams, B.J.; Chung, H.K.; Daniel, F.; Delahaye, F.; et al. The virtual atomic and molecular data centre (VAMDC) consortium. *J. Phys. B* **2016**, *49*, 074003. [CrossRef]
42. Albert, D.; Antony, B.K.; Ba, Y.A.; Babikov, Y.L.; Bollard, P.; Boudon, V.; Delahaye, F.; Del Zanna, G.; Dimitrijević, M.S.; Drouin, B.J.; et al. A Decade with VAMDC: Results and Ambitions. *Atoms* **2020**, *8*, 76. [CrossRef]
43. Rolader, G.E.; Batteh, J.H. Thermodynamic and electrical properties of railgun plasma armatures. *IEEE Trans. Plasma Sci.* **1989**, *17*, 439–445. [CrossRef]
44. Dimitrijević, M.S.; Djurić, Z.; Mihajlov, A.A. Stark broadening of Al III and Cu IV lines for diagnostic of the rail gun arc plasma. *J. Phys. D* **1994**, *27*, 247–252. [CrossRef]
45. Pakhal, H.R.; Lucht, R.P.; Laurendeau, N.M. Spectral measurements of incipient plasma temperature and electron number density during laser ablation of aluminum in air. *Appl. Phys. B* **2008**, *90*, 15–27. [CrossRef]